Influence of wastewater matrix on the visible light degradation of phenol using $AgCl/Bi_{24}O_{31}Cl_{10}$ photocatalyst

Dorcas O. Adenuga[*1], Shepherd M. Tichapondwa[1], Evans M.N. Chirwa[1]

*dorcasadenuga@yahoo.co.uk, shepherd.tichapondwa@up.ac.za, evans.chirwa@up.ac.za

[1]Water and Environmental Engineering Division, Department of Chemical Engineering, University of Pretoria, Pretoria 0002, South Africa.

Abstract

A significant amount of research has been conducted on the development and application of photocatalytic materials for the visible light degradation of organic pollutants in wastewater. However, most pollutant degradation studies are conducted using simulated wastewater often prepared using DI water. This is far removed from the realities of environmentally relevant water systems. It is therefore important to investigate the activity of these semiconductor materials with real water samples. In this study, the photocatalytic activity of the photocatalyst was investigated in the secondary effluent of a wastewater treatment plant (WWTP) in Pretoria, South Africa for the degradation of phenol under visible light irradiation. The experimental design was done using the Taguchi method L16 orthogonal tray with three factors (pH, initial phenol concentration and photocatalyst dosage) and four levels. The results show that pH is the highest-ranked significant factor influencing the degradation rate, closely followed by the initial concentration of the pollutant. The photocatalyst dosage had the least significant impact on degradation. The effects of individual anion components such as Cl^-, NO_3^-, NO_2^-, SO_4^{2-} and cations such as Ca^{2+}, Mg^{2+}, Zn^{2+} and K^+ were investigated. While Cl^- did not negatively influence the degradation rate, the results show that NO_3^- and SO_4^{2-} inhibit the degradation of phenol. More specifically, the presence of nitrites resulted in total impeding of the degradation process illustrating that nitrite concentrations ≥ 20 ppm should be removed from wastewater prior to photocatalytic degradation. The cations investigated promoted the degradation of phenol. Generally, there was enhanced degradation in the water matrix when compared to DI water and the results revealed improved degradation efficiency due to the cumulative impact of various components of the wastewater.

Keywords: degradation, photocatalysis, phenol, matrix effect, wastewater

Introduction

Photocatalysis continues to be applied in various environmental remediation as a green technique (Gao et al., 2022). Toxic pollutants such as phenolic compounds are harmful to human health when discharged into the environment due to their harmful properties of toxicity, carcinogenic behaviour and endocrine disrupting abilities (Sharma and Basu, 2020, Zulfiqar et al., 2019). Photocatalysis is a type of advanced oxidation process (AOP) that is regarded as a promising technology in the removal of organic contaminants in wastewater due to its efficiency, easy usage and good reproducibility (Zhu and Zhou, 2019, Wang et al., 2020b). It can oxidize organic pollutants using photogenerated reactive radicals, holes and electron transfer (Zhang et al., 2019). Previous studies used TiO_2 for the removal of toxic pollutants from wastewater because of its low cost and environmentally friendly properties (Šojić Merkulov et al., 2018). Its disadvantages are that it is activated for degradation only under UV light irradiation thereby making it ineffective for visible light irradiation (Kumar et al., 2021). UV light accounts for only 5% of solar energy while visible light is nearly 45% (Wang et al., 2020d). In the 21st century, research into the development of visible light photocatalysis has increased, as it is attractive for practical applications while utilizing naturally available resources. Different modification strategies are employed in the synthesis of visible–light-activated photocatalysts for improving their visible light activation characteristics. The band engineering strategies include creating heterojunctions through semiconductor coupling (Bera et al., 2019), metal (Wi et al., 2018), non-metallic (He et al., 2021) doping, plasmonic coupling (Adenuga et al., 2020, Li et al., 2020), and self-assembly amongst others. The intrinsic advantages of these strategies include wider light-harvesting efficiencies and hindered rate of charge combination thereby improving degradation and the visible-light activity of the photocatalyst (Tahir et al., 2020). In our earlier report, we showed that the deposition of AgCl nanoparticles on the surface of $Bi_{24}O_{31}Cl_{10}$ rods resulted in the enhanced degradation of two classes of pollutants, herbicide (2,4-dichlorophenoxy acetic acid) and antibiotic (tetracycline) (Adenuga et al., 2021). However, while the photocatalyst showed good efficiency in the degradation of single-component pollutants in de-ionized water, it is important to investigate the activity of the photocatalyst in a more complex matrix in order to investigate the effects of water components on catalyst effectiveness. Most wastewater matrix consists of various inorganic ions such as Na^+, K^+, Ca^{2+}, Mg^{2+}, SO_4^{2-}, HCO_3^-, Cl^-, NO_3^- and others (Tay, 2021) and they may influence the degradation rates of pollutants based on the amount of ions present (Gągol et al., 2020). Surface water and wastewater also consist of natural organic matter (NOM) which can influence photocatalytic activity through; (1) the formation of singlet and triplet states during irradiation and (2) the action of NOM components acting as filtering agents of photochemical light due to their lack of being photoinductive (Yuan et al., 2019). Since

important reactive oxygen species (ROS) are generated during photocatalytic degradation (Wang et al., 2015), they could be affected by components in a water matrix. This could stem from light attenuation, scavenging, formation of iron complexation, adsorption to a catalyst and less active radical formation and could be advantageous in the formation of ROS which acts as an additional catalyst source and aids the regeneration of photocatalyst (Lado Ribeiro et al., 2019).

In this study, previously synthesized photocatalyst AgCl/$Bi_{24}O_{31}Cl_{10}$ (Adenuga et al., 2021) was used in the degradation of phenol in wastewater matrix collected from the Daspoort Wastewater Treatment works in Pretoria, South Africa. It is one of the 10 WWTP in the Tshwane municipality and the effluent flows into the Apies River (Badejo et al., 2018). The secondary effluent from the local wastewater treatment plant was spiked with phenol. This contaminant was selected as a model pollutant for its chemical stability and persistence in wastewater bodies (Othman et al., 2019). It is also identified as a priority pollutant on the US EPA list (Lebedev et al., 2018). This research aimed to investigate the effects of inorganic ions of secondary effluents on the photoactivity of the as-synthesized photocatalyst. The conditions were analyzed optimally using the statistical analysis of the Taguchi method. Taguchi method uses a set of orthogonal arrays that enables the minimal number of experiments to cover all the parameters that will give the full information that influences the process (Nakhostin Panahi et al., 2021).

Experimental

Reagents

Phenol, glacial acetic acid, H_2SO_4, NaOH, and $NaNO_3$ were purchased from Glassworld, SA. $NaNO_2$, Na_2SO_4, $ZnSO_4.7H_2O$, $MgSO_4.7H_2O$ and NaCl were purchased from Merck SA. HPLC-grade acetonitrile was purchased from VWR chemicals. K_2SO_4 and $CaSO_4.0.5H_2O$ were purchased from SAARCHEM. Deionized water from an Elga PureLab Chorus unit was used except stated otherwise.

Catalyst synthesis and characterization

The photocatalyst used in this study was synthesized based on an established method described in our previous study (Adenuga et al., 2021). Briefly, prior studies established that 20%AgCl deposited on the surface of $Bi_{24}O_{31}Cl_{10}$ was optimal for 2,4-dichlorophenoxy acetic acid and 50%AgCl/$Bi_{24}O_{31}Cl_{10}$ for tetracycline degradation. In this work, 50%AgCl/$Bi_{24}O_{31}Cl_{10}$ was selected for the visible light degradation of phenol. The stoichiometric amount of AgCl was deposited on the surface of prepared $Bi_{24}O_{31}Cl_{10}$ using $AgNO_3$ and cetyltrimethylammonium chloride (CTAC). The samples were subsequently washed with ethanol and de-ionized

water before oven drying at 60ºC. The characteristics of the synthesized photocatalysts were investigated by scanning electron microscope (SEM) using a Zeiss Crossbeam 540 FEG SEM instrument, x-ray diffraction (XRD) was carried out on a PANalytical X'Pert Pro powder diffractometer, transmission electron microscope (TEM) was done using a JEOL JEM 2100F. The optical and photonic properties were investigated through UV-visible spectroscopy and photoluminescence (PL) using a VWR UV-1600PC spectrophotometer and a Shimadzu RF-6000 Spectro fluorophotometer.

Photocatalytic degradation

The photocatalytic degradation study was carried out in a photoreactor consisting of six 36W visible lamps arranged in pairs as depicted in Figure 1. 400 mL beakers were used as reactors with 200 mL of the aqueous solution being used. The concentration of phenol was varied from 5 mg/L to 30 mg/L while the catalyst dosage was varied from 0.25 g/L to 1 g/L. pH was adjusted using NaOH and H_2SO_4. Before exposure to visible light for 4 h, the solution was stirred by a magnetic stirrer for 30 min in the dark to reach adsorption-desorption equilibrium. 5 mL aliquots of the sample were withdrawn every 30 min. They were filtered using a 0.45 µm membrane filter before analysis.

Figure 1 Photocatalytic degradation set-up

Analytical methods

Phenol detection was done on a Waters 2998 PDA detector using a PAH C18 (4.6 x 250 nm, 5 µm) column. The mobile phase used was 30% 1% acetic in DI water and 70% acetic acid in acetonitrile with 280 nm absorption wavelength, 1.2 mL/min flow rate and injection volume of 10 µL. Inorganic ions were quantified using a 940

Professional IC varion ion chromatography (Metrohm, Herisau, Switzerland) with a separation column Metrosep C6-250/4.0 (Metrohm, Switzerland) and C 6 eluent 8 mM oxalic acid (Metrohm, Herisau, Switzerland).

Raw water source used in the experiments

The water samples were collected from the Daspoort wastewater treatment plant in Gauteng, South Africa. The effluent water was collected and analyzed. Table 1 shows the physical and chemical properties of the collected water. The samples were spiked with a well-known concentration of the previously prepared solution of phenol.

Table 1 The effluent characteristics of the Daspoort WWTP, Pretoria, South Africa

Parameters	**Value**
pH	7
Floride (mg/L)	0.21
Chloride (mg/L)	48.24
Nitrite (mg/L)	0.97
Bromide (mg/L)	0.15
Nitrate (mg/L)	14.11
Sulfate (mg/L)	56.70
Phosphate (mg/L)	0.39
Lithium (mg/L)	0.03
Sodium (mg/L)	54.79
Ammonium (mg/L)	9.27
Manganese (mg/L)	0.07
Magnesium (mg/L)	13.98
Potassium (mg/L)	11.71
Calcium (mg/L)	30.10
Strontium(mg/L)	0.08

Experimental design and Analysis of Variance (ANOVA)

Experimental design (DOE) was performed to determine the optimal conditions for degradation of phenol using $AgCl/Bi_{24}O_{31}Cl_{10}$ photocatalyst in an aqueous solution of spiked WWTP secondary effluent. The Taguchi L16(4^3)

method was applied while using the Minitab software. The "Larger is better" case was used for the Signal-to-noise (S/N) ratio to define the optimal conditions. The effects of pH, phenol concentration and photocatalyst dose were investigated with four levels in Table 2. The bigger is better function is determined by Eqs. (1):

$$S/N = -10 \log \left(\frac{1}{n}\sum_{i=1}^{n}\frac{1}{Y_i^2}\right) \quad (1)$$

Where S/N is the response average for each factor and Yi is the removal of the ith experiment. The degradation efficiency response as a function of time was calculated using Eqs. (2):

$$\text{Degradation efficiency } (\%) = \frac{(C_0 - C_t)}{C_0} \times 100 \quad (2)$$

Where C_0 and C_t are the concentrations of phenol at t = 0 and t respectively.

Table 2 Photodegradation factors and their levels using the Taguchi method

Factor	Level 1	Level 2	Level 3	Level 4
pH	3	5	7	9
Phenol concentration (mg/L)	5	10	20	30
Photocatalyst dose (g/L)	0.25	0.5	0.75	1

Results and discussion

Material characterization

The SEM images of the 50%AgCl/$Bi_{24}O_{31}Cl_{10}$ photocatalyst were depicted in Figures 2(a) and 2(b) and reveal that AgCl nanoparticles were deposited on the surface of rod-like $Bi_{24}O_{31}Cl_{10}$. Figure 2(c) confirms the deposition of the spherical-like particles on the surface of the $Bi_{24}O_{31}Cl_{10}$, further confirming the variation in particle morphology for the two compounds. In figure 2(d), the EDX spectra confirm the presence of the various elements (Ag, Cl, Bi and O) which make up the composite compounds in their expected ratios as reported in Adenuga et al., (2021). The purity and crystalline structure of the two photocatalysts were determined using XRD and the spectra are presented in Figure 2(e). Both materials were highly crystalline and pure $Bi_{24}O_{31}Cl_{10}$ is well indexed on the (JCPD NO. 75-0877) database (Kang et al., 2020). The presence of AgCl was confirmed by the peaks indexed at 30.8° and 37.7°. The extent of recombination of the photogenerated electron/hole pair was examined

in Figure 2(f). The PL intensity of the composite photocatalyst reduced compared to pure $Bi_{24}O_{31}Cl_{10}$ which had a high recombination rate. It can therefore be postulated that the coupling of the two compounds resulted in the formation of a heterojunction which in turn altered the charge transfer path leading to lowered electron/hole recombination (Ghattavi and Nezamzadeh-Ejhieh, 2020). UV-vis spectrophotometry was used to analyze the light absorption capacity of the photocatalyst at varying wavelengths. Figure 2(g) shows that while $Bi_{24}O_{31}Cl_{10}$ has a higher light absorption in the UV region, the AgCl deposited $Bi_{24}O_{31}Cl_{10}$ photocatalyst has a wider absorption in the visible light region. This was attributed to the plasmonic effect imparted by the AgCl nanoparticles. This observation suggests that the composite catalyst possesses superior visible light degradation efficiency (Adenuga et al., 2021).

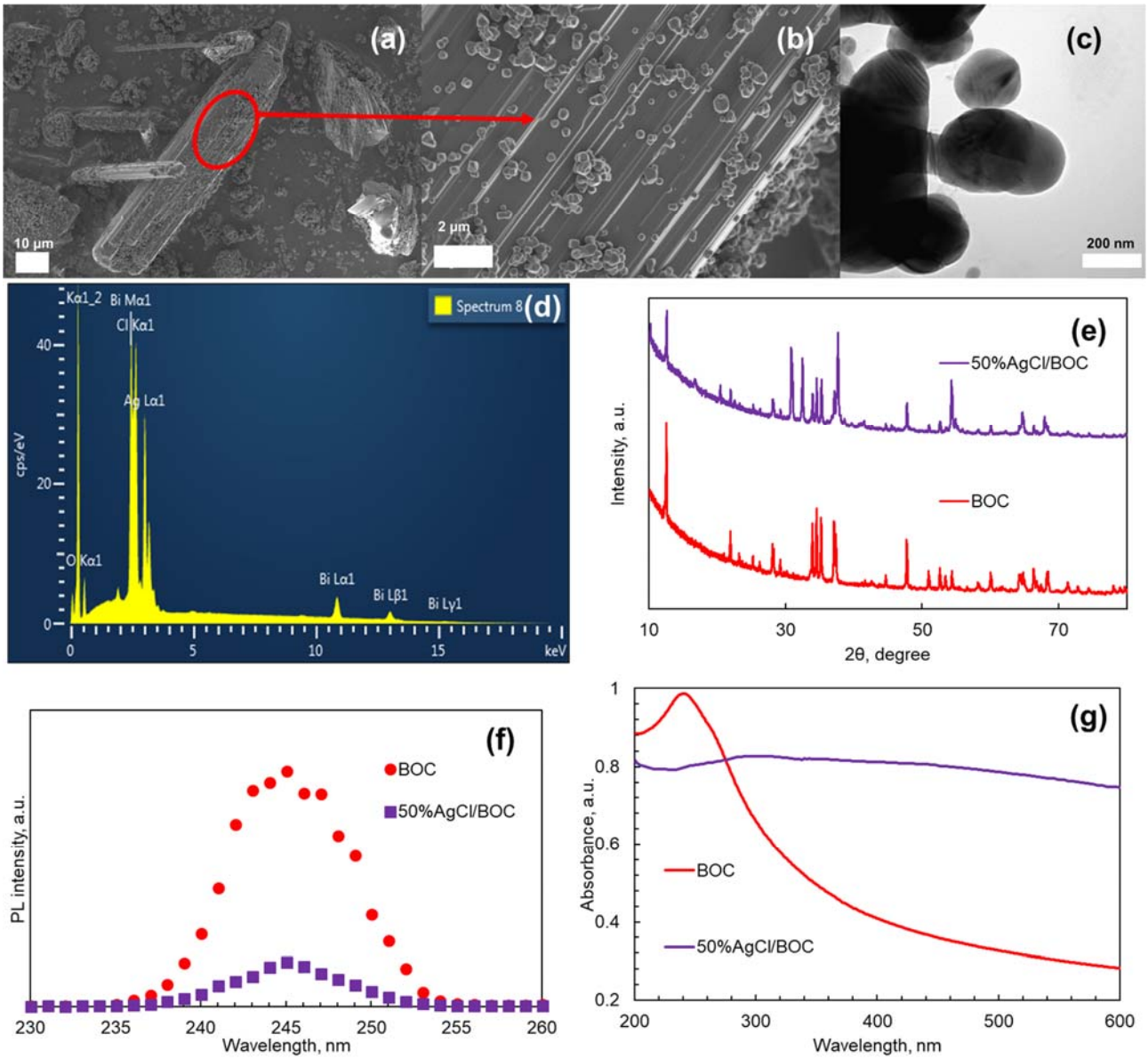

Figure 2 (a) Area- and (b) Zoomed-in view SEM image of 50% AgCl/$Bi_{24}O_{31}Cl_{10}$ (c) TEM of 50%AgCl/$Bi_{24}O_{31}Cl_{10}$, (d) SEM-EDX Spectra of 50%AgCl/$Bi_{24}O_{31}Cl_{10}$ (e) XRD Spectra of $Bi_{24}O_{31}Cl_{10}$ and 50%AgCl/$Bi_{24}O_{31}Cl_{10}$, (f) PL spectra of $Bi_{24}O_{31}Cl_{10}$ and 50%AgCl/$Bi_{24}O_{31}Cl_{10}$, (g) UV-VIS spectra of $Bi_{24}O_{31}Cl_{10}$ and 50%AgCl/$Bi_{24}O_{31}Cl_{10}$

Degradation studies

The degradation studies following the design of experiment and their responses are reported in Table 3 while the signal S/N ratio table for the larger is better case is shown in Table 4.

Table 3 Experimental design and response using Taguchi method L16

No	pH	Phenol Concentration (mg/L)	Photocatalyst dose (g/L)	Degradation (%)
1	3	5	0.25	7
2	3	10	0.5	2
3	3	20	0.75	2
4	3	30	1	6
5	5	5	0.5	57
6	5	10	0.25	13
7	5	20	1	7
8	5	30	0.75	9
9	7	5	0.75	80
10	7	10	1	53
11	7	20	0.25	11
12	7	30	0.25	20
13	9	5	1	84
14	9	10	0.75	50
15	9	20	0.5	23
16	9	30	0.25	10

Table 4 Order of parameters influencing the photocatalytic degradation of phenol

Level	pH	Phenol concentration	Photocatalyst dose
1	11.13	32.14	20.00
2	23.35	24.19	23.60
3	29.85	17.75	24.29
4	29.92	20.17	26.36
Delta	18.80	14.40	6.36
Rank	1	2	3

The results show that the most important factor determining the degradation efficiency of phenol is pH. The second-ranked factor is the initial phenol concentration and photocatalyst dosage ranks third. pH is an important factor affecting degradation rate due to its effects on the chemical properties of the pollutant, the surface of the photocatalyst and the reaction kinetics (Moradi et al., 2021). The photocatalytic degradation of phenol at an acidic aqueous solution of 3 using AgCl/$Bi_{24}O_{31}Cl_{10}$ photocatalyst was not supported. The concentration of hydroxyl ion reduces in an acidic medium due to the concentration of proton and this ion is required for the formation of hydroxyl radicals which might be a reactive species aiding degradation (Norouzi et al., 2020). Also, the effects of initial concentration were investigated between 5 mg/L and 30 mg/L. At the highest phenol concentrations of 30 mg/L, the degradation efficiency reported in the experiments was 20% or less while the highest degradation efficiencies were measured at lower concentrations. This phenomenon has been previously confirmed by other studies (Ahmadpour et al., 2020, Sayadi et al., 2019) as a possible increased interaction between the pollutant and the reactive species at lower pollutant concentration as compared to when the pollutant concentration is higher. This results in limited active sites available for photocatalysis to take place as more organic material is adsorbed on the surface of the photocatalyst material while a limited amount of photons reaches the surface of the photocatalyst (Rafiq et al., 2021). Therefore, the results present a potential for application in the removal of pollutants at low-level concentrations. In these experiments, while pH and initial contaminant concentration were of more significance, photocatalyst dosage is another factor that affects the photodegradation efficiency. Experiments 9 and 13 from Table 3 were carried out at photocatalyst dosages of 0.75 g/L and 1 g/L. High

photocatalyst dosage enhanced photodegradation through the presence of more reactive sites and the availability of radical's production (Zhao et al., 2018). It is also known that an excessive amount of photocatalyst will reduce the intensity of penetrating light hence reducing the rate of photodegradation (Kiwaan et al., 2020). Figure 3 illustrates the mean of S/N ratios and levels of the three factors investigated. The optimal phenol concentration value was at level 1, while that of pH and photocatalyst dosage was at level 3 and level 4, respectively. This suggests the optimum conditions for the photocatalytic degradation of phenol using the photocatalyst.

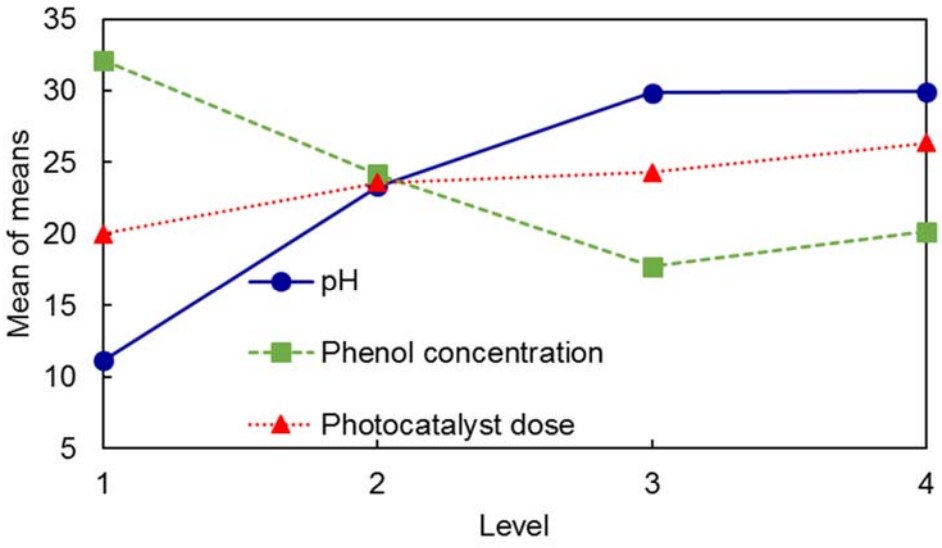

Figure 3 Main effects plots of means (pH, phenol concentration and photocatalyst dose)

The analysis of variance (ANOVA) was done to investigate the importance of the selected factors on the degradation of phenol and is reported in Table 5. Note that when P≤ 0.0001, highly significant; P≤ 0.01, strongly significant; P≤ 0.05, significant and when P> 0.05, not significant (Wang et al., 2019b). Based on Table 5 where the ANOVA results are shown and where DF = degree of freedom, SS = sum of square, MS =mean of square F-value = Fisher variation ratio and P-value = significant probability value, the P-values conclude that pH and phenol concentration are strongly significant factors for the removal of phenol in a waster matrix while the photocatalyst dosage was the least significant. The multivariate coefficient R^2 = 0.9643 which is greater than 0.95 shows that the model responds to a change in response value in the 96.43% range. The $R_{adj}^2 - R_{pred}^2$ = 0.9107 – 0.7459 = 0.1648 < 0.2 shows reliability of the experiments.

Table 5 Analysis of variance for the photocatalytic degradation of phenol

Source	DF	Adj SS	Adj MS	F-Value	P-Value
pH	3	3845.2	1281.75	18.27	0.002
Phenol Concentration	3	5673.3	1891.08	26.95	0.001
Photocatalyst dose	3	1844.2	614.75	8.76	0.013
Error	6	421.0	70.17		
Total	15	11783.7			

The general impact of the wastewater matrix was assessed in the degradation of phenol under visible light irradiation and is reported in Figure 4. Experiments were carried out under photolysis and adsorption conditions to investigate the individual effects of light and photocatalyst. The results show negligible degradation of phenol illustrating that light and photocatalysts are required for photocatalytic degradation to take place. After 4 h of light irradiation, photocatalytic degradation of phenol in DI water was 48% while in the water matrix from Daspoort effluent, phenol degradation (Experiment 9 in Table 3) was measured at 80%. In this case, the presence of ions promoted degradation when compared to the degradation efficiency in DI water. It is known that various dissolved components in water could either have promotion, inhibitory or neutral effects on the degradation efficiency (Lado Ribeiro et al., 2019). For practical applications, pH, the presence of ions and organics could affect the photocatalytic activity of the semiconductor (Zhao et al., 2019).

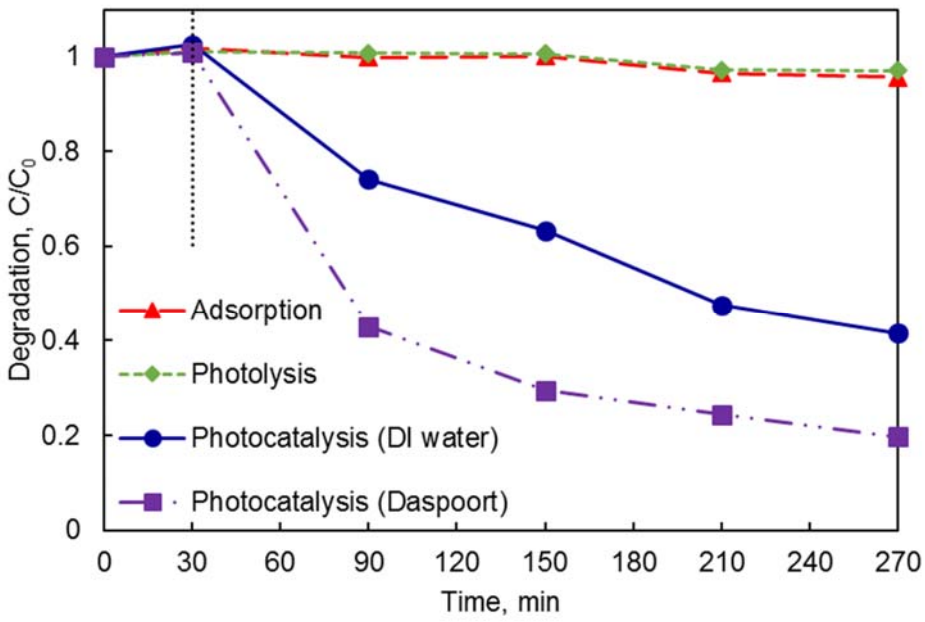

Figure 4 Degradation of phenol under different conditions of adsorption, photolysis, photocatalysis (DI and Daspoort water)

The pH of the effluent water enhanced the degradation of the organic pollutant using the photocatalyst. While the pH of the secondary effluent was 7, the pH of deionized water is 5.5. In Table 3, degradation at a pH condition below 7 is limited. Moreover, the interfering influence of anions such as Cl^-, SO_4^{2-}, NO_2^- and NO_3^- were selected to investigate the individual influence in DI water. The results of these interactions are reported in Figure 5. Sodium salts were used to avoid the various interaction of different cations. Na^+ is known to be at its maximum oxidation state in these salts and as such, will not compete as an h^+ scavenger and also does not influence the surface charge of the photocatalyst at concentrations less than 100 mM (Wang et al., 2015).

After the addition of SO_4^{2-} (Figure 5a), at a low sulfate concentration of 20 ppm, the degradation of phenol was neutral while at a higher concentration (50 ppm), there was a reduced effect in the degradation rate. Sulfate has the potential to be adsorbed on the surface of the photocatalysts while also interacting with the available holes and hydroxyl radicals (Raha and Ahmaruzzaman, 2020). It is important to investigate the effects of nitrates as they are always present in water bodies even at low concentrations. At high concentrations, it indicates the presence of water from sources such as livestock waste and could act as a hydroxyl radical to form $NO_3^{\bullet}$ which is less reactive (Eslami et al., 2020). The addition of nitrates to the photocatalytic reaction (Figure 5b) shows that it has an inhibition effect on the degradation efficiency of phenol after 4 h of light irradiation at both 20 and 50 ppm. The

degradation efficiency was reduced by 10% when nitrates were introduced. There was total inhibition of degradation when nitrite (Figure 5c) was introduced into the photocatalytic system at both 20 ppm and 50 ppm. Wang et al. (2020a) explain that in the presence of NO_2^- the transition n → π* of nitrite easily occurs and NO_2^- is oxidized to $HNO_3\bullet^-$ or $(NO_3\bullet)^{2-}$ radical species by the •OH radicals and as such the hydroxyl radicals are not available for degradation. Therefore, for the practical application of phenol removal from wastewater using the photocatalyst, nitrite should be removed before implementing photocatalysis. The wastewater investigated in this study had 0.97 mg/L nitrite present and this could have been too little to effectively inhibit the degradation rate.

Figure 5d shows the effects of chloride ions on the degradation of phenol. Cl^- shows a reduction in degradation efficiency in the range of 3% - 6% on the degradation of phenol using $AgCl/Bi_{24}O_{31}Cl_{10}$ as a photocatalyst. Additional Cl^- in the solution has the potential of forming inorganic free radicals Cl• and $Cl_2\bullet^-$ which are also reactive and could promote the degradation of phenol (Wang et al., 2018). Photocatalytic degradation involving Ag/AgCl – based photocatalysts has reported that Cl• takes part in the degradation process due to its strong oxidizing potential (Wang et al., 2020c, Wu et al., 2019). The concentration of chloride ions in the WWTP effluent used in this study was 48 mg/L and would have had an almost negligible effect on the degradation efficiency.

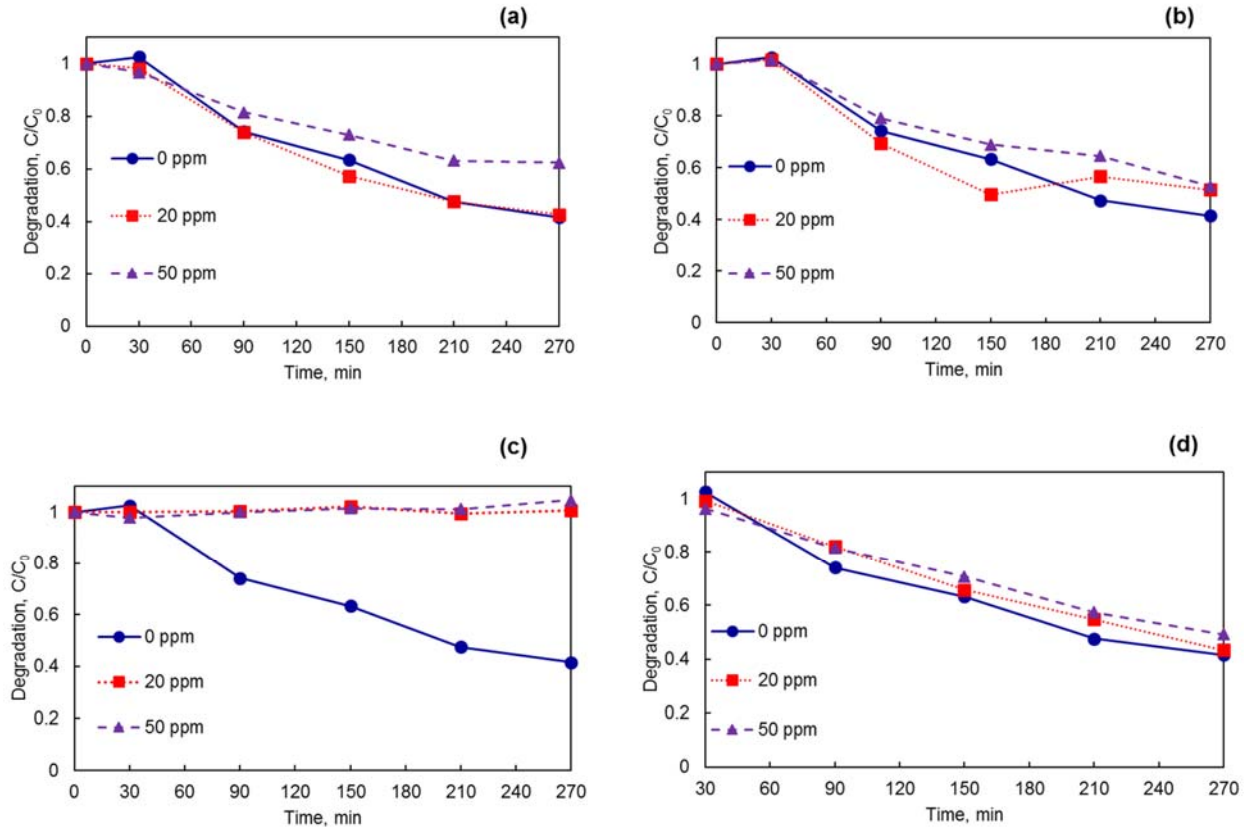

Figure 5 Influence of various ions in the removal of phenol (a) SO_4^{2-}, (b) NO_3^-, (c) NO_2^- and (d) Cl^-

Sulfate salts of potassium (K_2SO_4), zinc ($ZnSO_4.7H_2O$), calcium ($CaSO_4.0.5H_2O$) and magnesium ($MgSO_4.7H_2O$) were used at concentrations of 20 mg/L and 50 mg/L to investigate the effects of cations in wastewater for the photodegradation of organic pollutants under the same conditions and reported in Figure 6(a)-(d). Although it has been previously suggested that these metal ions should not affect degradation as they are already in a stable oxidation state (Dugandžić et al., 2017), the results show that the presence in the wastewater proposes promotion effects to degradation. Cations present in the wastewater effluent investigated include magnesium, potassium and calcium at concentrations of 13.98, 11.71 and 30.10 mg/L respectively. The results show that the summative effects of these ions promoted the degradation efficiency in the water matrix in comparison to DI water. He et al. (2019) confirm that cations such as Ca^{2+} enhance the adsorption of carbamazepine on the surface of the photocatalyst BiOCl thereby improving the degradation efficiency.

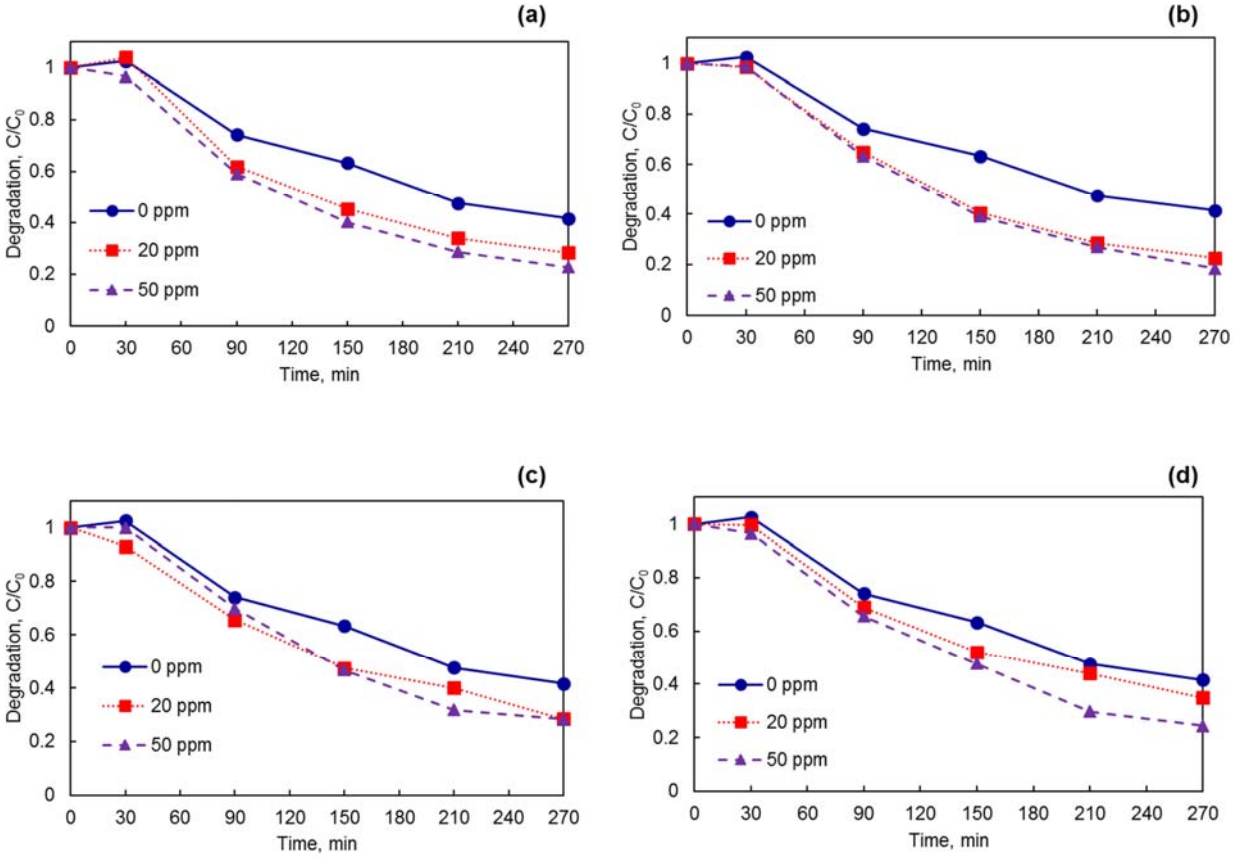

Figure 6 Influence of various ions in the removal of phenol (a) Mg^{2+}, (b) Ca^{2+}, (c) Zn^{2+} and (d) K^{+}

Catalyst stability

The reusability of the photocatalyst in the degradation of phenol was estimated through three consecutive cycles. After each cycle, the photocatalysts were collected and washed with deionized water to remove pollutants from the surface of the photocatalyst. The material was then dried in an oven for 60 °C prior to the next cycle. The recycling experiments were carried out in similar conditions to experiment 9 in Table 3.

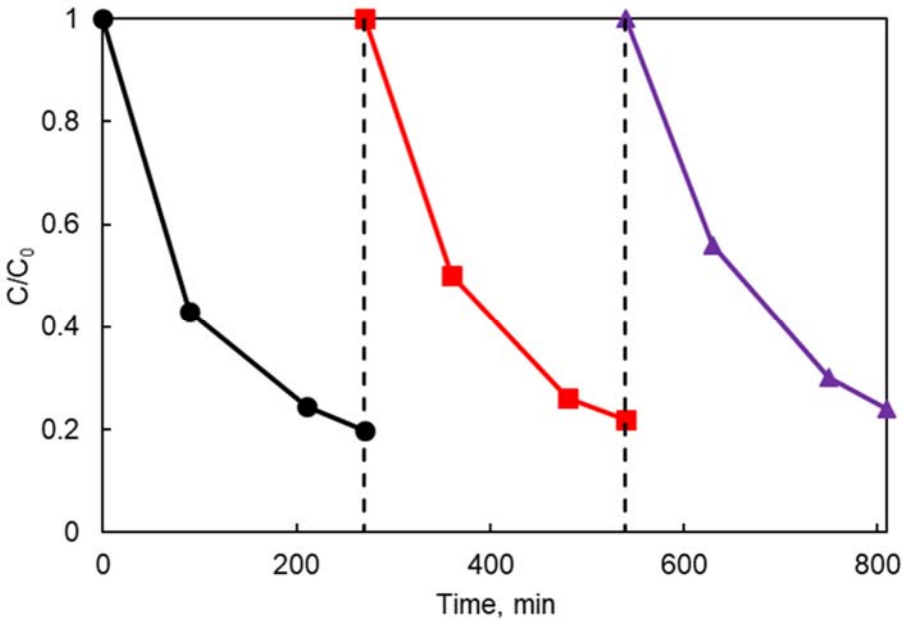

Figure 7 Successive photocatalytic degradation of phenol by $AgCl/Bi_{24}O_{31}Cl_{10}$ under visible light irradiation

As shown in Figure 7, the degradation efficiency reduced from 80% in cycle 1 to 75% in cycle 3. This points to the relative stability and reusability of the synthesized composite photocatalyst. This agrees with other studies where AgCl-based photocatalysts have been utilized. Raizada et al., (2020) in their study examined the stability of their photocatalyst BiOBr/PSCN/Ag/AgCl in the degradation of phenol and measured a reduction of 98% to 90% even after seven cycles. In the evaluation performance of $Ag/AgCl@Ti^{3+}\text{-}TiO_2$ for the degradation of tetracycline, Yu et al., (2021) in their study also identify that no inactivation phenomenon is recorded and the slight reduction in activity after three cycles could be attributed to the loss of material or the leaching of Ag from the composite. It should be noted that the material was easily separated from the suspension which also bodes well with its recyclability.

Comparison with previous studies on the degradation of pollutants in wastewater

Lei et al. (2020) in their study investigated the antibiotics degradation rate in the presence of water matrices. They found that Cl^- and SO_4^{2-} act as radical scavengers and can absorb photons at 245 nm and as such reduce the degradation rate of the antibiotics. Wang et al. (2020e) in their work proved that divalent cations (Mg^{2+} and Ca^{2+}) improved the removal efficiency of Naproxen. This is because these identified cations improved the absorption of the pollutant on the surface of the photocatalyst. In the photodegradation of levofloxacin using a ternary magnetic photocatalyst Ag_3PO_4/rGO/$CoFe_2O_4$ (Hu et al., 2021), Cl^- reduced the degradation efficiency due to its adsorptive competition with the pollutants on the photocatalyst surface while sulfates had zero effect on the degradation rate. Jiménez-Salcedo et al. (2021) compared the photocatalytic degradation of sodium diclofenac using g-C_3N_4 nanosheets in both ultrapure water and tap water under visible light and natural sunlight conditions. Under both light conditions, their result shows a higher degradation of sodium diclofenac in tap water as compared to ultrapure water and the cause was attributed to the presence of "chloride ions of salts".

When investigating the effect of water quality on the degradation of tetracycline while using BVO/FTO@rGO photocatalysts, Yang et al. (2020) report a decrease in degradation in the presence of SO_4^{2-}, Cl^- and CO_3^- while the degradation was promoted only in the presence of Cr^{6+}. Their work proposes that while Cr^{6+} and tetracycline consume electrons and holes, recombination is inhibited thereby promoting degradation. The anions consume free radicals while also converting them to radicals with lesser oxidizing power thereby reducing the photodegradation efficiency. In the removal of phenolic contaminants using bismuth-modified TiO_2 photocatalyst (Tang et al., 2021), phenol degradation was still achieved in the presence of $CaCl_2$, NaCl and KCl while the degradation rate of phenol decreased in the presence of inorganic anions (Cl^-, HCO_3^- and SO_4^{2-}).

It is noted that while each component of the water matrix will have its individual effects, the components tend to balance each other thereby having a general effect on degradation or mineralization rate (Náfrádi et al., 2021). Other studies reporting the effects of inorganic ions on the degradation of recalcitrant pollutants are reported in Table 6.

Table 7 shows the degradation of phenol using various photocatalysts under different reaction conditions. Parameters such as pH, light source, and initial pollutant concentration have been shown to influence the rate of degradation. For example, Chang et al., (2018) measured the highest degradation efficiency in an acidic condition of pH 2 in the presence of Fe_2O_4/TiO_2 while Moradi et al., (2021) has an optimal pH of 8 when using $FeTiO_3$/GO

photocatalyst. Studies carried out using different light sources have shown that excellent degradation efficiency is measured in photocatalytic degradation carried out under UV and high wattage visible light irradiation in a shorter period. It is known that the rate of degradation increases with a decrease in wavelength and therefore shorter wavelength leads to quicker degradation (Ahmad et al., 2020). Galedari et al., (2016) degraded 96% of 50 mg/L phenol in 120 min using UVC light irradiation with a ZnO@SiO_2 photocatalyst while 41% of the same concentration was degraded in 420 min when using ZnO/Ag_2CO_3/Ag_2O in Rosman et al., (2018) study. Hayati and co-workers (2018) degraded phenol at 60 mg/L initial concentration in 160 min using ZnO/TiO_2@rGO photocatalyst while Mohamed et al., (2019) degraded a lower concentration (10 mg/L) in a shorter period of 20 min using PAN-CNT/TiO_2-NH_2 photocatalyst. In our study, low-wattage visible light was used to simulate the degradation experiments. For potential practical application, photocatalytic materials that can be activated under low-wattage light and natural sunlight are preferred.

Table 6 Summary of different photocatalysts reported for the degradation of organic pollutants in the presence of different ions in wastewater/real-water samples

Photocatalysts	**Pollutant**	**Promoted effect**	**Neutral Effect**	**Inhibited effect**	**Reference**
Co_3O_4-Bi_2O_3	Bisphenol A	High Cl^-	-	H_2PO_4 and CO_3^{2-}	(Hu et al., 2018)
UV/TiO_2	Metronidazole	Glucose	-	Fe^{3+}, H_2PO_4, Ca^{2+}, Mg^{2+}, Cl^-, SO_4^{2-}, NO_3^-, HCO_3^-	(Tran et al., 2019)
UVA-LED/TiO_2/persulfate	Ibuprofen	-	-	Cl-, SO_4^{2-}, HCO_3^-	(Ding and Hu, 2020)
g-C_3N_4/$Bi_2O_2CO_3$	Tetracycline	-	-	Cl^-, NO_3^-, CO_3^{2-}, SO_4^{2-}, Mg^{2+}, Fe^{3+}, NH_4^+, Zn^{2+}, Ca^{2+}	(Zhao et al., 2019)
AgI/UiO-66	Sulfamethoxazole	-	SO_4^{2-} and Cl^-	HCO_3^-	(Wang et al., 2018)
TiO_2	Sulfamethoxazole	-	-	HPO_4^{2-}, HCO_3^-, SO_4^{2-}, Cl^-, $H_2PO_4^-$	(Yuan et al., 2019)
CQDs/g-C_3N_4	Sulfamethazine	HCO_3^-			(Di et al., 2020)
Cu-CNF/MLCT	CTC-HCl	-	Na^+, K^+	Zn^{2+}, Mg^{2+}, NO_2^-	(Wang et al., 2020a)
NCD_s/TNS-001	DCF	-	Cl^-, SO_4^{2-}, Mg^{2+},	Fe^{3+}, Cu^{2+}	(Wang et al., 2019a)
$Cu_{0.84}Bi_{2.08}O_4$/PDS/Visible light	CIP	-	-	HCO_3^-, PO_4^{3-}, SO_4^{2-}, NO_3^-,	(Tang et al., 2019)
NCD_s-BiOBr/CeO_2	CBZ			SO_4^{2-}, NO_3^-,	(Liang et al., 2020)
$FeTiO_3$/GO	Phenol	-	-	HCO_3^-, Cl^-, SO_4^{2-}	(Moradi et al., 2021)

CeO_2/IK-C_3N4	Acetaminophen	-	-	Cl^-, NO_3^-, SO_4^{2-}, PO_4^{3-}	(Paragas et al., 2021)
Bi_2O_3-Sensitized TiO_2	Tetracycline	-	Cl^-	SO_4^{2-}, NO_3^-	(Shi et al., 2020)
2D-Bi_4NbO_8Cl	Tetracycline	-	-	CO_3^{2-}, Cl^-, SO_4^{2-}	(Majumdar et al., 2022)
CuO-Cu_2O	Methylene Blue	Low Cl^-	-	SO_4^{2-}, High Cl^-, NO_3^-	(Tavakoli Joorabi et al., 2022)
Floating porous g-C_3N_4	Tetracycline	Cl^-, SO_4^{2-}	-	-	(Tang et al., 2022)
AgCl/$Bi_{24}O_{31}Cl_{10}$	Phenol	Mg^{2+}, Ca^{2+}, Zn^{2+}, K^+	Cl^-	NO_3^-, NO_2^-, SO_4^{2-},	This study

Table 7 Comparison of the photocatalytic degradation of phenol with other studies

Photocatalyst	Initial phenol concentration (mg/L)	Light source	pH	Degradation efficiency	Degradation time	Reference
$FeTiO_3$/GO	50	150 W Xenon lamp	8	100%	150 min	(Moradi et al., 2021)
NCN/Bi_2WO_6	10	300 W Xenon lamp	-	93.1%	5 h	(Zhu and Zhou, 2020)
MgO@Ag/TiO_2	15	150 W Oriel Sol1A system	-	95%	120 min	(Scott et al., 2019)
BiOI/Bi_2WO_6	50	500 W Xenon lamp	-	90.27%	3 h	(Huang et al., 2021)
Fe_3O_4/TiO_2	100	18 W UV	2	99%	150 min	(Chang et al., 2018)
ZnO/TiO_2@rGO	60	150 W Vis	4	91%	160 min	(Hayati et al., 2018)
ZnO/Ag_2CO_3/Ag_2O	50	100 W Vis	-	41%	420 min	(Rosman et al., 2018)
PAN-CNT/TiO_2-NH_2	10	100 W Halogen lamp	5	99.7%	20 min	(Mohamed et al., 2019)
Ag/Ag_3PO_4/WO_3	10	300 W Xenon lamp	7	99%	150 min	(Shi et al., 2019)

$ZnO@SiO_2$	50	Three 16 W UVC lamps	5.9	96%	120 min	(Galedari et al., 2016)
$AgCl/Bi_{24}O_{31}Cl_{10}$	5	Six 36 W Visible lamps	9	84%	240 min	This study

Conclusions

In summary, the current work was carried out to evaluate the photocatalytic performance of $AgCl/Bi_{24}O_{31}Cl_{10}$ photocatalyst in the degradation of phenol in a secondary effluent from a wastewater treatment plant. The effects of three factors namely pH, initial pollutant concentration and photocatalyst dosage were investigated. The results show that pH is a dominant factor in the photodegradation process, followed by the concentration of pollutants and lastly, the photocatalyst dosage. The performance in the secondary effluent was better when compared to DI water. This was ascribed to the promoting effects of the pH and the presence of ions and other matter in the water matrix. While some ions have promoting effects, others are neutral or inhibit the degradation rate. As such, the total degradation rate is a cumulative response of all the various factors with some weighing more than the other.

Statements and Declaration

Funding Financial support from the National Research Foundation of South Africa (Grant numbers: MND190514436254, TTK18024324064, CSUR180215313534) was awarded to Dorcas Adenuga, Prof. Shepherd Tichapondwa and Prof. Evans Chirwa.

Author contributions Conceptualization, methodology, investigation and original draft writing by Dorcas Adenuga. Conceptualization, resources, editing, review, funding acquisition and supervision by Shepherd Tichapondwa and Evans Chirwa.

Data availability All data related to this manuscript is incorporated in the manuscript.

Ethics approval Not applicable.

Consent to participate All authors have approved the final version of the manuscript and have given their consent for publication.

Competing interests The authors declare no competing interests.

References

ADENUGA, D., SKOSANA, S., TICHAPONDWA, S. & CHIRWA, E. 2021. Synthesis of a plasmonic AgCl and oxygen-rich Bi24O31Cl10 composite heterogeneous catalyst for enhanced degradation of tetracycline and 2,4-dichlorophenoxy acetic acid. *RSC Advances,* 11**,** 36760-36768.

ADENUGA, D. O., TICHAPONDWA, S. M. & CHIRWA, E. M. N. 2020. Facile synthesis of a Ag/AgCl/BiOCl composite photocatalyst for visible – light – driven pollutant removal. *Journal of Photochemistry and Photobiology A: Chemistry,* 401**,** 112747.

AHMAD, K., GHATAK, H. R. & AHUJA, S. M. 2020. A review on photocatalytic remediation of environmental pollutants and H2 production through water splitting: A sustainable approach. *Environmental Technology & Innovation,* 19.

AHMADPOUR, N., SAYADI, M. H., SOBHANI, S. & HAJIANI, M. 2020. Photocatalytic degradation of model pharmaceutical pollutant by novel magnetic TiO2@ZnFe2O4/Pd nanocomposite with enhanced photocatalytic activity and stability under solar light irradiation. *Journal of Environmental Management,* 271**,** 110964.

BADEJO, A. A., OMOLE, D. O. & NDAMBUKI, J. M. 2018. Municipal wastewater management using Vetiveria zizanioides planted in vertical flow constructed wetland. *Applied Water Science,* 8.

BERA, S., WON, D.-I., RAWAL, S. B., KANG, H. J. & LEE, W. I. 2019. Design of visible-light photocatalysts by coupling of inorganic semiconductors *Catalysis Today,* 335.

CHANG, J., ZHANG, Q., LIU, Y., SHI, Y. & QIN, Z. 2018. Preparation of Fe3O4/TiO2 magnetic photocatalyst for photocatalytic degradation of phenol. *Journal of Materials Science: Materials in Electronics,* 29**,** 8258-8266.

DI, G., ZHU, Z., DAI, Q., ZHANG, H., SHEN, X., QIU, Y., HUANG, Y., YU, J., YIN, D. & KÜPPERS, S. 2020. Wavelength-dependent effects of carbon quantum dots on the photocatalytic activity of g-C3N4 enabled by LEDs. *Chemical Engineering Journal,* 379**,** 122296.

DING, H. & HU, J. 2020. Degradation of ibuprofen by UVA-LED/TiO2/persulfate process: Kinetics, mechanism, water matrix effects, intermediates and energy consumption. *Chemical Engineering Journal,* 397**,** 125462.

DUGANDŽIĆ, A. M., TOMAŠEVIĆ, A. V., RADIŠIĆ, M. M., ŠEKULJICA, N. Ž., MIJIN, D. Ž. & PETROVIĆ, S. D. 2017. Effect of inorganic ions, photosensitisers and scavengers on the photocatalytic degradation of nicosulfuron. *Journal of Photochemistry and Photobiology A: Chemistry,* 336**,** 146-155.

ESLAMI, A., MEHDIPOUR, F., LIN, K.-Y. A., SHARIFI MALEKSARI, H., MIRZAEI, F. & GHANBARI, F. 2020. Sono-photo activation of percarbonate for the degradation of organic dye: The effect of water matrix and identification of by-products. *Journal of Water Process Engineering,* 33.

GĄGOL, M., CAKO, E., FEDOROV, K., SOLTANI, R. D. C., PRZYJAZNY, A. & BOCZKAJ, G. 2020. Hydrodynamic cavitation based advanced oxidation processes: Studies on specific effects of inorganic acids on the degradation effectiveness of organic pollutants. *Journal of Molecular Liquids,* 307.

GALEDARI, N. A., RAHMANI, M. & TASBIHI, M. 2016. Preparation, characterization, and application of ZnO@SiO2 core–shell structured catalyst for photocatalytic degradation of phenol. *Environmental Science and Pollution Research,* 24**,** 12655-12663.

GAO, Y., FANG, X., CHEN, D., MA, N. & DAI, W. 2022. Ternary photocatalyst of ZIF-8 nanofilms coupled with AgI nanoparticles seamlessly on ZnO microrods for enhanced visible-light photocatalysis degradation. *Journal of the Taiwan Institute of Chemical Engineers,* 131**,** 104146.

GHATTAVI, S. & NEZAMZADEH-EJHIEH, A. 2020. A visible light driven AgBr/g-C3N4 photocatalyst composite in methyl orange photodegradation: Focus on photoluminescence, mole ratio, synthesis method of g-C3N4 and scavengers. *Composites Part B: Engineering,* 183.

HAYATI, F., ISARI, A. A., FATTAHI, M., ANVARIPOUR, B. & JORFI, S. 2018. Photocatalytic decontamination of phenol and petrochemical wastewater through ZnO/TiO2 decorated on reduced graphene oxide nanocomposite: influential operating factors, mechanism, and electrical energy consumption. *RSC Advances,* 8**,** 40035-40053.

HE, D., LUO, Y., PENG, W., TANG, G., GUO, Q. & GAO, X. 2019. Effects of inorganic ions on the photocatalytic degradation of carbamazepine. *Journal of Water Reuse and Desalination,* 9**,** 301-309.

HE, X., WU, M., AO, Z., LAI, B., ZHOU, Y., AN, T. & WANG, S. 2021. Metal–organic frameworks derived C/TiO2 for visible light photocatalysis: Simple synthesis and contribution of carbon species. *Journal of Hazardous Materials,* 403**,** 124048.

HU, L., ZHANG, G., LIU, M., WANG, Q. & WANG, P. 2018. Enhanced degradation of Bisphenol A (BPA) by peroxymonosulfate with Co3O4-Bi2O3 catalyst activation: Effects of pH, inorganic anions, and water matrix. *Chemical Engineering Journal,* 338**,** 300-310.

HU, Z., GE, M. & GUO, C. 2021. Efficient removal of levofloxacin from different water matrices via simultaneous adsorption and photocatalysis using a magnetic Ag3PO4/rGO/CoFe2O4 catalyst. *Chemosphere,* 268**,** 128834.

HUANG, X., GUO, Q., YAN, B., LIU, H., CHEN, K., WEI, S., WU, Y. & WANG, L. 2021. Study on photocatalytic degradation of phenol by BiOI/Bi2WO6 layered heterojunction synthesized by hydrothermal method. *Journal of Molecular Liquids,* 322**,** 114965.

JIMÉNEZ-SALCEDO, M., MONGE, M. & TENA, M. T. 2021. The photocatalytic degradation of sodium diclofenac in different water matrices using g-C3N4 nanosheets: A study of the intermediate by-products and mechanism. *Journal of Environmental Chemical Engineering,* 9**,** 105827.

KANG, J., JIN, C., LI, Z., WANG, M., CHEN, Z. & WANG, Y. 2020. Dual Z-scheme MoS2/g-C3N4/Bi24O31Cl10 ternary heterojunction photocatalysts for enhanced visible-light photodegradation of antibiotic. *Journal of Alloys and Compounds,* 825.

KIWAAN, H. A., ATWEE, T. M., AZAB, E. A. & EL-BINDARY, A. A. 2020. Photocatalytic degradation of organic dyes in the presence of nanostructured titanium dioxide. *Journal of Molecular Structure,* 1200.

KUMAR, R., RAIZADA, P., VERMA, N., HOSSEINI-BANDEGHARAEI, A., THAKUR, V. K., LE, Q. V., NGUYEN, V.-H., SELVASEMBIAN, R. & SINGH, P. 2021. Recent advances on water disinfection using bismuth based modified photocatalysts: Strategies and challenges. *Journal of Cleaner Production,* 297**,** 126617.

LADO RIBEIRO, A. R., MOREIRA, N. F. F., LI PUMA, G. & SILVA, A. M. T. 2019. Impact of water matrix on the removal of micropollutants by advanced oxidation technologies. *Chemical Engineering Journal,* 363**,** 155-173.

LEBEDEV, A. T., POLYAKOVA, O. V., MAZUR, D. M., ARTAEV, V. B., CANET, I., LALLEMENT, A., VAITILINGOM, M., DEGUILLAUME, L. & DELORT, A. M. 2018. Detection of semi-volatile compounds in cloud waters by GCxGC-TOF-MS. Evidence of phenols and phthalates as priority pollutants. *Environ Pollut,* 241**,** 616-625.

LEI, J., CHEN, B., ZHOU, L., DING, N., CAI, Z., WANG, L., IN, S.-I., CUI, C., ZHOU, Y., LIU, Y. & ZHANG, J. 2020. Efficient degradation of antibiotics in different water matrices through the photocatalysis of inverse opal K-g-C3N4: Insights into mechanism and assessment of antibacterial activity. *Chemical Engineering Journal,* 400**,** 125902.

LI, M., LI, D., ZHOU, Z., WANG, P., MI, X., XIA, Y., WANG, H., ZHAN, S., LI, Y. & LI, L. 2020. Plasmonic Ag as electron-transfer mediators in Bi2MoO6/Ag-AgCl for efficient photocatalytic inactivation of bacteria. *Chemical Engineering Journal,* 382**,** 122762.

LIANG, L., GAO, S., ZHU, J., WANG, L., XIONG, Y., XIA, X. & YANG, L. 2020. The enhanced photocatalytic performance toward carbamazepine by nitrogen-doped carbon dots decorated on BiOBr/CeO2: Mechanism insight and degradation pathways. *Chemical Engineering Journal,* 391**,** 123599.

MAJUMDAR, A., GHOSH, U. & PAL, A. 2022. 2D-Bi4NbO8Cl nanosheet for efficient photocatalytic degradation of tetracycline in synthetic and real wastewater under visible-light: Influencing factors, mechanism and degradation pathway. *Journal of Alloys and Compounds,* 900**,** 163400.

MOHAMED, A., NASSER, W. S., KAMEL, B. M. & HASHEM, T. 2019. Photodegradation of phenol using composite nanofibers under visible light irradiation. *European Polymer Journal,* 113**,** 192-196.

MORADI, M., VASSEGHIAN, Y., KHATAEE, A., HARATI, M. & ARFAEINIA, H. 2021. Ultrasound-assisted synthesis of FeTiO3/GO nanocomposite for photocatalytic degradation of phenol under visible light irradiation. *Separation and Purification Technology,* 261**,** 118274.

NÁFRÁDI, M., ALAPI, T., BENCSIK, G. & JANÁKY, C. 2021. Impact of Reaction Parameters and Water Matrices on the Removal of Organic Pollutants by TiO2/LED and ZnO/LED Heterogeneous Photocatalysis Using 365 and 398 nm Radiation. *Nanomaterials,* 12**,** 5.

NAKHOSTIN PANAHI, P., MOHAJER, S. & RASOULIFARD, M. H. 2021. Photocatalytic of Congo Red Decolorization in the Presence of Ag/AgCl/TiO2 Nanocomposite: Optimization of Process with Taguchi Method. *Arabian Journal for Science and Engineering,* 46**,** 5619-5632.

NOROUZI, M., FAZELI, A. & TAVAKOLI, O. 2020. Phenol contaminated water treatment by photocatalytic degradation on electrospun Ag/TiO2 nanofibers: Optimization by the response surface method. *Journal of Water Process Engineering,* 37**,** 101489.

OTHMAN, I., ABU HAIJA, M., ISMAIL, I., ZAIN, J. H. & BANAT, F. 2019. Preparation and catalytic performance of CuFe2O4 nanoparticles supported on reduced graphene oxide (CuFe2O4/rGO) for phenol degradation. *Materials Chemistry and Physics,* 238.

PARAGAS, L. K. B., DIEN DANG, V., SAHU, R. S., GARCIA-SEGURA, S., DE LUNA, M. D. G., PIMENTEL, J. A. I. & DOONG, R.-A. 2021. Enhanced visible-light-driven photocatalytic degradation of acetaminophen over CeO2/I, K-codoped C3N4 heterojunction with tunable properties in simulated water matrix. *Separation and Purification Technology,* 272**,** 117567.

RAFIQ, A., IKRAM, M., ALI, S., NIAZ, F., KHAN, M., KHAN, Q. & MAQBOOL, M. 2021. Photocatalytic degradation of dyes using semiconductor photocatalysts to clean industrial water pollution. *Journal of Industrial and Engineering Chemistry,* 97**,** 111-128.

RAHA, S. & AHMARUZZAMAN, M. 2020. Enhanced performance of a novel superparamagnetic g-C3N4/NiO/ZnO/Fe3O4 nanohybrid photocatalyst for removal of esomeprazole: Effects of reaction parameters, co-existing substances and water matrices. *Chemical Engineering Journal,* 395**,** 124969.

RAIZADA, P., THAKUR, P., SUDHAIK, A., SINGH, P., THAKUR, V. K. & HOSSEINI-BANDEGHARAEI, A. 2020. Fabrication of dual Z-scheme photocatalyst via coupling of BiOBr/Ag/AgCl heterojunction with P and S co-doped g-C3N4 for efficient phenol degradation. *Arabian Journal of Chemistry,* 13**,** 4538-4552.

ROSMAN, N., SALLEH, W. N. W., ISMAIL, A. F., JAAFAR, J., HARUN, Z., AZIZ, F., MOHAMED, M. A., OHTANI, B. & TAKASHIMA, M. 2018. Photocatalytic degradation of phenol over visible light active ZnO/Ag2CO3/Ag2O nanocomposites heterojunction. *Journal of Photochemistry and Photobiology A: Chemistry,* 364**,** 602-612.

SAYADI, M. H., SOBHANI, S. & SHEKARI, H. 2019. Photocatalytic degradation of azithromycin using GO@Fe3O4/ ZnO/ SnO2 nanocomposites. *Journal of Cleaner Production,* 232**,** 127-136.

SCOTT, T., ZHAO, H., DENG, W., FENG, X. & LI, Y. 2019. Photocatalytic degradation of phenol in water under simulated sunlight by an ultrathin MgO coated Ag/TiO2 nanocomposite. *Chemosphere,* 216**,** 1-8.

SHARMA, S. & BASU, S. 2020. Highly reusable visible light active hierarchical porous WO3/SiO2 monolith in centimeter length scale for enhanced photocatalytic degradation of toxic pollutants. *Separation and Purification Technology,* 231**,** 115916.

SHI, H., YANG, S., HAN, C., NIU, Z., LI, H., HUANG, X. & MA, J. 2019. Fabrication of Ag/Ag3PO4/WO3 ternary nanoparticles as superior photocatalyst for phenol degradation under visible light irradiation. *Solid State Sciences,* 96**,** 105967.

SHI, Q., ZHANG, Y., SUN, D., ZHANG, S., TANG, T., ZHANG, X. & CAO, S. 2020. Bi2O3-Sensitized TiO2 Hollow Photocatalyst Drives the Efficient Removal of Tetracyclines under Visible Light. *Inorganic Chemistry,* 59**,** 18131-18140.

ŠOJIĆ MERKULOV, D. V., DESPOTOVIĆ, V. N., BANIĆ, N. D., ARMAKOVIĆ, S. J., FINČUR, N. L., LAZAREVIĆ, M. J., ČETOJEVIĆ-SIMIN, D. D., ORČIĆ, D. Z., RADOIČIĆ, M. B., ŠAPONJIĆ, Z. V., ČOMOR, M. I. & ABRAMOVIĆ, B. F. 2018. Photocatalytic decomposition of selected biologically active compounds in environmental waters using TiO2/polyaniline nanocomposites: Kinetics, toxicity and intermediates assessment. *Environmental Pollution,* 239**,** 457-465.

TAHIR, M., TASLEEM, S. & TAHIR, B. 2020. Recent development in band engineering of binary semiconductor materials for solar driven photocatalytic hydrogen production. *International Journal of Hydrogen Energy,* 45**,** 15985-16038.

TANG, H., DAI, Z., XIE, X., WEN, Z. & CHEN, R. 2019. Promotion of peroxydisulfate activation over Cu0.84Bi2.08O4 for visible light induced photodegradation of ciprofloxacin in water matrix. *Chemical Engineering Journal,* 356**,** 472-482.

TANG, J., WANG, J., TANG, L., FENG, C., ZHU, X., YI, Y., FENG, H., YU, J. & REN, X. 2022. Preparation of floating porous g-C3N4 photocatalyst via a facile one-pot method for efficient photocatalytic elimination of tetracycline under visible light irradiation. *Chemical Engineering Journal,* 430**,** 132669.

TANG, W., CHEN, J., YIN, Z., SHENG, W., LIN, F., XU, H. & CAO, S. 2021. Complete removal of phenolic contaminants from bismuth-modified TiO2 single-crystal photocatalysts. *Chinese Journal of Catalysis,* 42**,** 347-355.

TAVAKOLI JOORABI, F., KAMALI, M. & SHEIBANI, S. 2022. Effect of aqueous inorganic anions on the photocatalytic activity of CuO–Cu2O nanocomposite on MB and MO dyes degradation. *Materials Science in Semiconductor Processing,* 139**,** 106335.

TAY, C. K. 2021. Hydrogeochemical framework of groundwater within the Asutifi-North District of the Brong-Ahafo Region, Ghana. *Applied Water Science,* 11.

TRAN, M. L., FU, C.-C. & JUANG, R.-S. 2019. Effects of water matrix components on degradation efficiency and pathways of antibiotic metronidazole by UV/TiO2 photocatalysis. *Journal of Molecular Liquids,* 276**,** 32-38.

WANG, C., XUE, Y., WANG, P. & AO, Y. 2018. Effects of water environmental factors on the photocatalytic degradation of sulfamethoxazole by AgI/UiO-66 composite under visible light irradiation. *Journal of Alloys and Compounds,* 748**,** 314-322.

WANG, D., LI, Y., LI PUMA, G., WANG, C., WANG, P., ZHANG, W. & WANG, Q. 2015. Mechanism and experimental study on the photocatalytic performance of Ag/AgCl @ chiral TiO2 nanofibers photocatalyst: The impact of wastewater components. *Journal of Hazardous Materials,* 285**,** 277-284.

WANG, F., WU, Y., WANG, Y., LI, J., JIN, X., ZHANG, Q., LI, R., YAN, S., LIU, H., FENG, Y., LIU, G. & LV, W. 2019a. Construction of novel Z-scheme nitrogen-doped carbon dots/{0 0 1} TiO2 nanosheet photocatalysts for broad-spectrum-driven diclofenac degradation: Mechanism insight, products and effects of natural water matrices. *Chemical Engineering Journal,* 356**,** 857-868.

WANG, H., ZHANG, J., YUAN, X., JIANG, L., XIA, Q. & CHEN, H. 2020a. Photocatalytic removal of antibiotics from natural water matrices and swine wastewater via Cu(I) coordinately polymeric carbon nitride framework. *Chemical Engineering Journal,* 392**,** 123638.

WANG, J., ZHANG, Q., DENG, F., LUO, X. & DIONYSIOU, D. D. 2020b. Rapid toxicity elimination of organic pollutants by the photocatalysis of environment-friendly and magnetically recoverable step-scheme SnFe2O4/ZnFe2O4 nano-heterojunctions. *Chemical Engineering Journal,* 379**,** 122264.

WANG, N., CHENG, K., XU, Z.-F., LI, P., GENG, G., CHEN, C., WANG, D., CHEN, P. & LIU, M. 2020c. High-performance natural-sunlight-driven Ag/AgCl photocatalysts with a cube-like morphology and blunt edges via a bola-type surfactant-assisted synthesis. *Physical Chemistry Chemical Physics,* 22**,** 3940-3952.

WANG, N., LI, X., YANG, Y., SHANG, Y., ZHUANG, X., LI, H. & ZHOU, Z. 2019b. Combined process of visible light irradiation photocatalysis-coagulation enhances natural organic matter removal: Optimization of influencing factors and mechanism. *Chemical Engineering Journal,* 374**,** 748-759.

WANG, Q., GAO, Q., AL-ENIZI, A. M., NAFADY, A. & MA, S. 2020d. Recent advances in MOF-based photocatalysis: environmental remediation under visible light. *Inorganic Chemistry Frontiers,* 7**,** 300-339.

WANG, Y., JING, B., WANG, F., WANG, S., LIU, X., AO, Z. & LI, C. 2020e. Mechanism Insight into enhanced photodegradation of pharmaceuticals and personal care products in natural water matrix over crystalline graphitic carbon nitrides. *Water Research,* 180**,** 115925.

WI, D. H., PARK, S. Y., LEE, S., SUNG, J., HONG, J. W. & HAN, W. H. 2018. Metal–semiconductor ternary hybrids for efficient visible-light photocatalytic hydrogen evolution. *Journal of Materials Chemistry A,* 6**,** 13225.

WU, W., WANG, J., ZHANG, T., JIANG, S., MA, X., ZHANG, G., ZHANG, X., CHEN, X. & LI, B. 2019. Controllable synthesis of Ag/AgCl@MIL-88A via in situ growth method for morphology-dependent photocatalytic performance. *Journal of Materials Chemistry C,* 7**,** 5451-5460.

YANG, R., ZHU, Z., HU, C., ZHONG, S., ZHANG, L., LIU, B. & WANG, W. 2020. One-step preparation (3D/2D/2D) BiVO4/FeVO4@rGO heterojunction composite photocatalyst for the removal of tetracycline and hexavalent chromium ions in water. *Chemical Engineering Journal,* 390**,** 124522.

YU, X., HUANG, J., ZHAO, J., LIU, S., XIANG, D., TANG, Y., LI, J., GUO, Q., MA, X. & ZHAO, J. 2021. Efficient visible light photocatalytic antibiotic elimination performance induced by nanostructured Ag/AgCl@Ti3+-TiO2 mesocrystals. *Chemical Engineering Journal,* 403.

YUAN, R., ZHU, Y., ZHOU, B. & HU, J. 2019. Photocatalytic oxidation of sulfamethoxazole in the presence of TiO2: Effect of matrix in aqueous solution on decomposition mechanisms. *Chemical Engineering Journal,* 359**,** 1527-1536.

ZHANG, Z., BAI, L., LI, Z., QU, Y. & JING, L. 2019. Review of strategies for the fabrication of heterojunctional nanocomposites as efficient visible-light catalysts by modulating excited electrons with appropriate thermodynamic energy. *Journal of Materials Chemistry A,* 7**,** 10879.

ZHAO, H., LI, G., TIAN, F., JIA, Q., LIU, Y. & CHEN, R. 2019. g-C3N4 surface-decorated Bi2O2CO3 for improved photocatalytic performance: Theoretical calculation and photodegradation of antibiotics in actual water matrix. *Chemical Engineering Journal,* 366**,** 468-479.

ZHAO, X., DU, P., CAI, Z., WANG, T., FU, J. & LIU, W. 2018. Photocatalysis of bisphenol A by an easy-settling titania/titanate composite: Effects of water chemistry factors, degradation pathway and theoretical calculation. *Environ Pollut,* 232**,** 580-590.

ZHU, D. & ZHOU, Q. 2019. Action and mechanism of semiconductor photocatalysis on degradation of organic pollutants in water treatment: A review. *Environmental Nanotechnology, Monitoring & Management,* 12**,** 100255.

ZULFIQAR, M., SAMSUDIN, M. F. R. & SUFIAN, S. 2019. Modelling and optimization of photocatalytic degradation of phenol via TiO2 nanoparticles: An insight into response surface methodology and artificial neural network. *Journal of Photochemistry and Photobiology A: Chemistry,* 384.